Pergamon

Acta mater. Vol. 46, No. 16, pp. 5663–5675, 1998
© 1998 Acta Metallurgica Inc.
Published by Elsevier Science Ltd. All rights reserved
Printed in Great Britain
PII: S1359-6454(98)00252-3
1359-6454/98 $19.00 + 0.00

TRANSFORMATION SUPERPLASTICITY OF SUPER α_2 TITANIUM ALUMINIDE

C. SCHUH and D. C. DUNAND†

Department of Materials Science and Engineering, Northwestern University, Evanston, IL 60208, U.S.A.

(Received 15 May 1998; accepted 7 July 1998)

Abstract—Transformation superplasticity of an intermetallic Ti_3Al-based alloy (Super α_2) is demonstrated by thermal cycling about the α_2/β transformation temperature range under a uniaxial tensile biasing stress. Failure strains up to 610% were recorded at a stress of 3 MPa, compared with 110% for deformation by isothermal creep at the same stress. The strain increment produced during each half-cycle is determined as a function of applied biasing stress, thermal cycle amplitude, and cycling frequency. Since internal stresses are generated both by transformation mismatch and by thermal expansion mismatch between the two coexisting phases, an effective volume mismatch is defined to account for both contributions. Introduction of this parameter into existing continuum-mechanics models results in good agreement with experimental data in both the low-stress regime, where cycling strain rate and stress are proportional, and the high-stress regime where the stress sensitivity is increasing. Cycling strain increments at various temperature amplitudes and cycling frequencies are considered in terms of the equilibrium thermodynamics and transformation kinetics of Super α_2. Finally, thermal cycling produces ratcheting, where texture and crystallographic orientation of the β/α_2 transformation front affect the direction of ratcheting strains. © *1998 Acta Metallurgica Inc. Published by Elsevier Science Ltd. All rights reserved.*

1. INTRODUCTION

Internal-stress plasticity is a deformation phenomenon observed in crystalline solids upon generation of internal stress in the presence of an external biasing stress [1, 2]. Internal stresses can be created by a polymorphic phase transformation between two phases of different density. The transformation mismatch stresses are biased in the direction of the applied external stress and deformation occurs by a mechanism such as time-independent plastic yield (e.g. Fe [3, 4], Co [3, 5]) or time-dependent creep (e.g. Ti [3, 6], Zr [3, 7]). In the absence of a biasing stress, an excursion through the transformation range and back results in no net deformation of the material, except when a sharp transformation front exists, as for thermal ratcheting of uranium [8, 9]. However, application of an external load biases internal mismatch stresses, resulting in a finite, irreversible strain increment on each thermal cycle about the transformation range. These strain increments can often be accumulated without fracture to tensile strains in excess of 100%, a phenomenological requirement for transformation superplasticity [1, 2].

Greenwood and Johnson [3] developed a widely accepted continuum-mechanics model of transformation superplasticity which predicts a linear relationship between the plastic strain increment produced after each transformation, $\Delta\varepsilon$, and the externally-applied biasing stress, σ. For the case of a material relaxing internal stresses by creep, they derived the following expression, valid only at low applied stresses ($\sigma \ll \sigma_o$):

$$\Delta\varepsilon \approx \frac{2}{3} \cdot \frac{\Delta V}{V} \cdot \frac{\sigma}{\sigma_o} \cdot \frac{5 \cdot n}{(4 \cdot n + 1)} \tag{1}$$

where $\Delta V/V$ is the volume mismatch between the two phases, σ_o is the time- and space-averaged internal stress in the weaker phase during a full transformation, and n is the stress exponent for creep of the weaker phase. Because transformation superplasticity does not require grain boundary sliding (as does microstructural superplasticity), polymorphic materials with large grain sizes and with stress exponents larger than unity under isothermal conditions can be deformed to very large strains under thermal cycling conditions [7].

The model of Greenwood and Johnson was extended by Mitter [10] to larger applied stresses, where the relationship between the biased transformation strain increment, $\Delta\varepsilon$, and the applied stress, σ, is given by:

$$\delta = \frac{3}{2} \cdot \overline{\left[(\eta - \gamma) \cdot \left(1 + \frac{9}{4} \cdot \eta^2 - \frac{9}{2} \cdot \eta \cdot \gamma \right)^{(1-n)/2 \cdot n} \right]} \tag{2}$$

where the bar notation indicates an average over a spherical volume element and the dimensionless values η, δ, and γ are defined as [7, 10]:

†To whom all correspondence should be addressed.

$$\eta \equiv \frac{\Delta\varepsilon}{\Delta V/V} \tag{3a}$$

$$\delta \equiv \frac{\sigma}{\sigma_o} \tag{3b}$$

$$\gamma \equiv \frac{(\Delta V/V)_{zz}}{\Delta V/V} \tag{3c}$$

with σ as the biasing stress in the z-direction and $(\Delta V/V)_{zz}$ the zz-component of the volume mismatch tensor. The volume integral of equation (2) cannot, in general, be solved in closed form, and so must be solved numerically for a given strain increment and stress exponent [7, 10]. At low applied stresses, this model approaches the linear relationship given by equation (1).

Transformation plasticity can potentially be exhibited by any material which undergoes a solid state phase transformation with a non-zero volume mismatch, $\Delta V/V$. It has been studied in pure metals [3, 5, 7], alloys (steel [11], Ti–6Al–4V [12, 13]), metal matrix composites [6, 13, 14], ceramics [15], and ceramic matrix composites [16]. We are aware of only two studies on transformation plasticity of intermetallic-based materials. Zwigl and Dunand [17] investigated the intermetallic matrix composite NiAl/ZrO_2, where the transformation of the ceramic reinforcement enhanced the creep deformation of the non-transforming intermetallic matrix. While the material obeyed equation (1), relatively small failure strains ($< 25\%$) were reached because of fracture at the sample heads. Hornbogen and Wassermann [18] examined the compressive and tensile behavior of intermetallic β-brass under repeated formation of a martensitic phase. Because of work-hardening during thermal cycling, they achieved only about 2% total strain under a constant applied stress. To the best of our knowledge, no study to date has demonstrated transformation superplasticity of an intermetallic compound, under tensile stress and with failure strains greater than 100%.

Ti_3Al-based intermetallics are considered good candidates for high-temperature structural applications, but their technological implementation is hindered by their low ductility at low temperatures [19]. Superplastic deformation is thus of considerable interest for these and other intermetallics which present difficulties for traditional forming methods. In the present work, we demonstrate transformation superplasticity of a Ti_3Al-based intermetallic alloy (Super α_2) and characterize its superplastic strain increment in terms of applied stress and thermal cycle amplitude and frequency.

2. EXPERIMENTAL PROCEDURE

Sheets of 3 mm thick Super α_2 titanium aluminide with nominal composition Ti–25Al–10Nb–3Mo–1V (at.%) were acquired from Sulzer Innotec, Switzerland. In the as-received state [Fig. 1(a)], the material exhibits a two-phase microstructure typical of rolled Ti_3Al-based alloys, with approximately equal fractions of α_2 and β/B2 phases [20, 21]. Flat tensile specimens were electro-discharge machined with gauge length of 18 mm parallel to the rolling direction, and surface oxide was removed by light polishing.

Prior to dilatometry and high-temperature mechanical tests, all specimens were annealed in argon for 75 min at 1150°C (well within the β-field of this alloy) to promote the evolution of a large β grain structure [22]. Dilatometry was performed in vacuum with a Quenching and Deformation Dilatometer (from MMC, Westbury, New York) at a scan rate of 10 K/min. Creep and thermal cycling experiments were performed in a custom-built creep frame described in Ref. [7]. The apparatus allowed a controlled atmosphere of high-purity argon

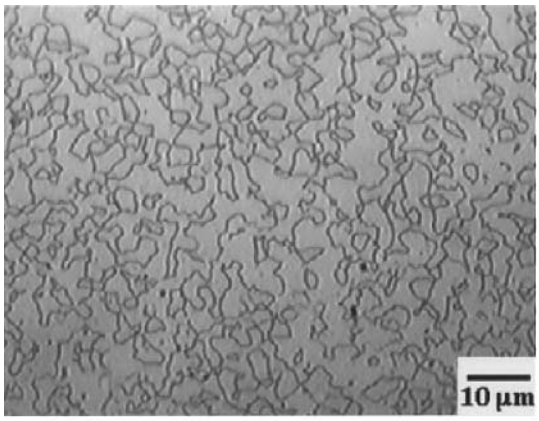

(a)

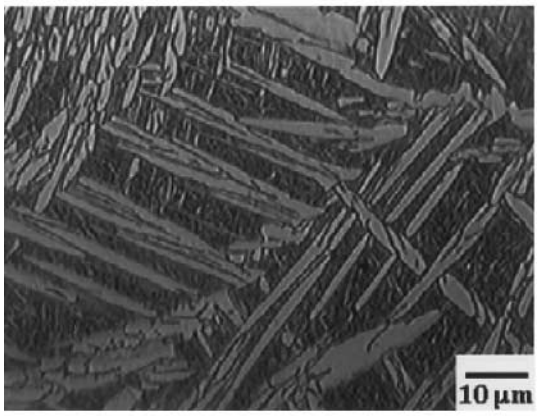

(b)

Fig. 1. Optical micrographs of Super α_2 (a) in the as-received state, and (b) after β-transformation at 1150°C (75 min), cooling to 950°C at about 5 K/s, annealing at that temperature (30 min) and room-temperature quenching. Light phase is the α_2 phase.

(99.999% pure, further gettered by titanium powder at about 1000°C), application of small stresses, and rapid heating by radiant furnaces. The sample temperature was controlled to within 5 K of the set-point by a molybdenum-sheathed, R-type thermocouple near the sample surface, except during some large-amplitude thermal cycles, where the lower cycling temperature was occasionally more than 5 K below the set-point for a brief time (short compared to the cycle time). The accuracy of the R-type thermocouple was confirmed up to 1000°C with a K-type thermocouple in contact with the specimen gauge.

Isothermal creep experiments were performed under conditions of decreasing temperature and increasing stress, with sufficient time allowed at any given stress and temperature for the measurement of a steady-state creep rate (SSCR). Prior to thermal cycling, each tensile specimen was isothermally crept at 1150°C until steady state was established, in order to eliminate any contribution of primary creep to cycling strains. Thermal cycling experiments were performed with varying stress and thermal cycle profiles. Rapid radiant heating with a closed-loop temperature controller resulted in nearly square thermal cycles (temperature ramps on the order of 20 s duration) for all cycle amplitudes and frequencies investigated. Four sets of thermal cycling experiments were performed:

1. Cycles between 950 and 1150°C were applied to investigate dependence of strain increments on stress in the range $\sigma = 0$–5 MPa with cycling frequency $\nu = 10$/h.
2. Strain increments were measured as a function of cycling frequency in the range $\nu = 4.28$–15/h between 950 and 1150°C with $\sigma = 2.0$ MPa.
3. Temperature amplitude was varied with constant $\sigma = 2.6$ MPa and $\nu = 10$/h. The upper cycle temperature, T_u, was maintained at 1150°C while the temperature amplitude was varied in the range $\Delta T = 50$–375 K.
4. One specimen was tested to failure with thermal cycles of $\nu = 10$/h between 950 and 1150°C. The true stress was maintained at 3.0 ± 0.1 MPa up to 150% engineering strain, after which true stress could no longer be accurately determined due to slight inhomogeneity of the specimen cross-section. At this point, the stress was adjusted to maintain a roughly uniform average deformation rate until failure occurred. One tensile specimen was isothermally crept to failure at 3.0 MPa and 1150°C for comparison.

In order to ascertain equilibrium microstructures, two as-received samples were subjected to different heat-treatment schedules. Each specimen was β-annealed at 1150°C for 75 min, followed by either quenching in ice water or cooling at about 5 K/s to 950°C (below the β-transus) where it was maintained at constant temperature for 30 min before further quenching in ice water. Metallographic preparation consisted of mechanical grinding, polishing with diamond paste, and brief immersion-etching in Kroll's reagent.

3. RESULTS

The as-received microstructure of Super α_2 [Fig. 1(a)] is fine and equiaxed, and has been demonstrated to exhibit microstructural superplasticity at temperatures in the two-phase $\alpha_2+\beta$ field (920–1040°C) [23–27]. However, the sample heat treated above the β-transus (75 min at 1150°C) and water quenched exhibited extremely coarse grains of β phase (around 1 mm). Figure 1(b) shows the microstructure of the specimen which was β-transformed, cooled to 950°C, and held for 30 min to guarantee an equilibrium microstructure [28, 29]. This microstructure is typical of α_2 aluminides after β-transformation and cooling without working in the $\alpha_2+\beta$ field [30, 31], and is composed of prior β-grains [which are too large to be seen in Fig. 1(b)] and Widmanstätten plates or laths of α_2. The large β grain size and the non-equiaxed morphology of α_2 plates inhibit cooperative sliding/rotation of grains, so that microstructural superplasticity can be ruled out for all β-transformed specimens used in the present study.

Figure 2 shows the dilatometric data of Super α_2 between 75 and 450°C, with a coefficient of thermal expansion (CTE) in this range of $\alpha_{75-450°C} = 1.00 \times 10^{-5}$/K. Liao *et al.* [32] reported thermal dilatation of Super α_2 to temperatures above the β-transus, but without specifying units of dilatation. However, the similarity of their material to that of the present study allows us to deduce the length

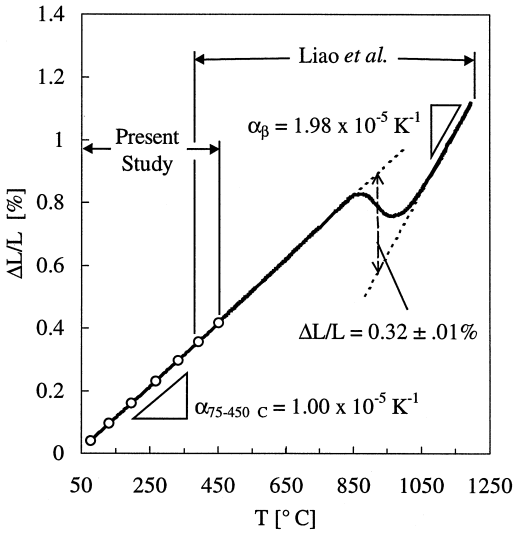

Fig. 2. Dilatation of Super α_2 alloy between 50 and 1250°C. Data with open circles are from the present study (10 K/min), superimposed upon data of Liao *et al.* (2 K/min) [32].

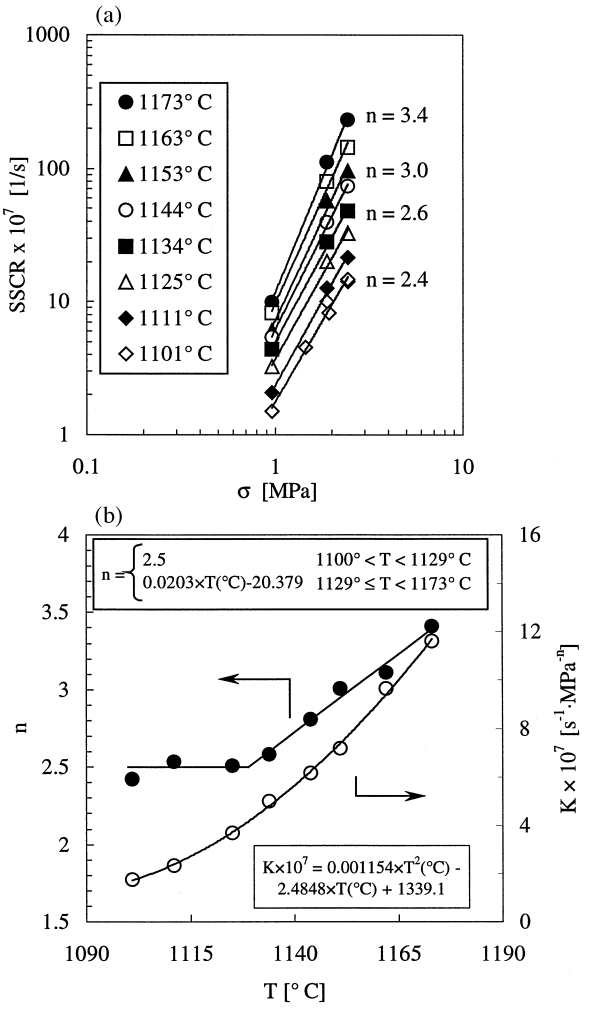

Fig. 3. Creep of Super α_2 above the β-transus: (a) stress dependence of steady-state creep rate (SSCR); (b) temperature dependence of creep parameters n and K [equation (4)], determined for σ (MPa) and SSCR (/s).

changes of their specimen based on $\alpha_{75-450°C}$. In Fig. 2 their data are fitted to $\alpha_{75-450°C}$ found in the present study over the range T = 350–450°C.

The SSCR of Super α_2 above the β-transus (reported in Ref. [29] as 1100°C) is presented as a function of the applied stress in Fig. 3(a). The stress exponent n ranges from about 2.4 to 3.4 between 1100 and 1170°C, the temperature range of interest to this study [Fig. 3(b)]. With this variable stress exponent, the creep behavior in this temperature range can be modeled by a simplified power-law equation:

$$\dot{\varepsilon} = K \cdot \sigma^n \tag{4}$$

where $\dot{\varepsilon}$ is the SSCR and K is a temperature-dependent variable which accounts for the activation energy and other variables in the full form of the power-law equation [33]. The temperature dependence of K is also shown in Fig. 3(b).

Creep data for temperatures below the β-transus are presented in Fig. 4. In Fig. 4(a), the SSCR is normalized by the bulk diffusion coefficient [24], $D\,[\mathrm{m}^2/\mathrm{s}] = 5.9 \times 10^{-3} \cdot \exp(-330000/R \cdot T)$, where R is the gas constant and T the absolute temperature. In the temperature range investigated here (950–1050°C), the material is composed of both β and α_2 phases, and the creep stress exponent is found to be very near unity. With n = 1 in this temperature regime, a diffusional creep equation [33] can be used to describe the SSCR:

$$\dot{\varepsilon} = \frac{A}{T} \cdot \sigma \cdot \exp\left(-\frac{Q}{R \cdot T}\right) \tag{5}$$

where Q is the creep activation energy and A is a constant incorporating atomic volume and grain size. The temperature dependence of SSCR is shown in Fig. 4(b), and indicates Q = 300 kJ/mol and A = 209 K/(Pa · s) for creep of the two-phase microstructure.

The total plastic strain increment ($\Delta\varepsilon_{tot}$) after a half thermal cycle between 950 and 1150°C at a frequency ν = 10/h is plotted as a function of

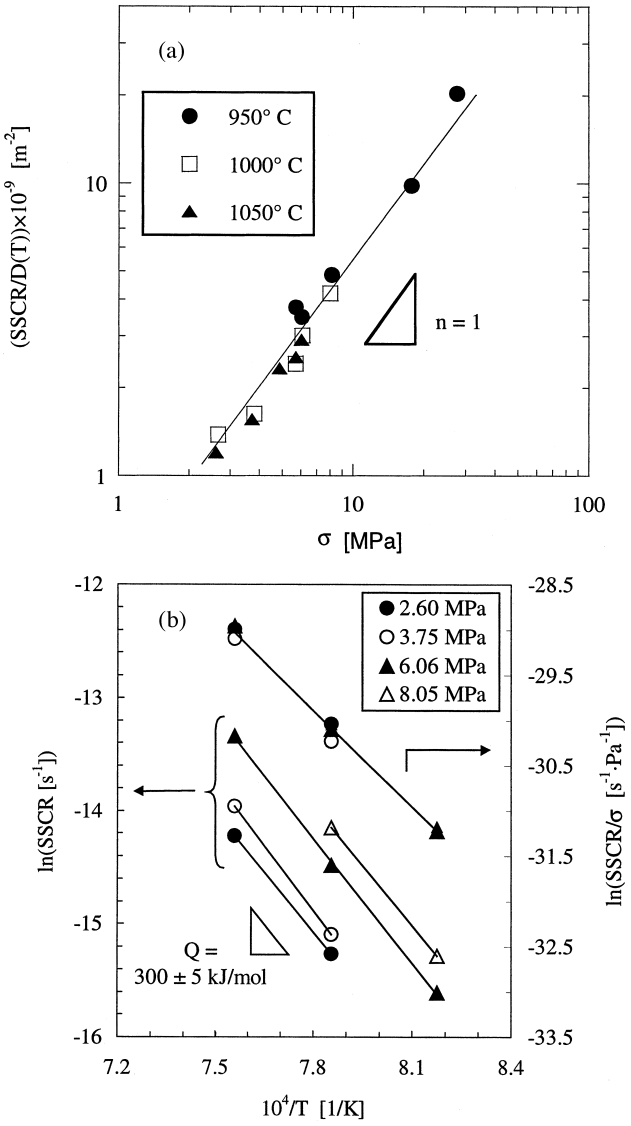

Fig. 4. Creep behavior of Super α_2 below the β-transus: (a) stress dependence of steady-state creep rate (SSCR) (solid line is not a best-fit); (b) temperature dependence of SSCR.

applied biasing stress in Fig. 5. This strain increment is found by measuring the plastic strain after a complete thermal cycle and assuming equal contributions to deformation from the heating and cooling half-cycles, following Ref. [3]. At low stresses, the stress is proportional to the total strain increment per transformation ($d(\Delta\varepsilon_{tot})/d\sigma = 0.77 \pm 0.05$/GPa), while at stresses above about 2 MPa an increasing stress sensitivity is observed. The temperature amplitude dependence of the effective cycling strain rate, $\dot{\varepsilon}_{tot}$ (equal to $2{\cdot}\Delta\varepsilon_{tot}{\cdot}\nu$), for cycles with $\nu = 10$/h and $\sigma = 2.6$ MPa is shown in Fig. 6, with a reference point of isothermal creep at 1150°C, where $\dot{\varepsilon} = 1.54 \times 10^{-5}$/s. The total effective strain rates at temperature amplitudes in the range $\Delta T = 225$–275 K were higher than the SSCR at 1150°C, with a maximum effective rate of 1.70×10^{-5}/s for $\Delta T = 250$ K. The effect of cycling frequency on $\Delta\varepsilon_{tot}$ is shown in Fig. 7 for cycles between 950 and 1150°C with $\sigma = 2.0$ MPa.

Specimens deformed to failure under comparable stress of 3.0 MPa are shown in Fig. 8. While the crept specimen failed with a total engineering strain $\varepsilon_f = 110\%$, the thermally cycled specimen reached $\varepsilon_f = 610\%$ after 612 cycles between 950 and 1150°C at a frequency $\nu = 10$/h.

4. DISCUSSION

4.1. Thermal dilatation and volume mismatch

Although there is an abundance of generally consistent crystallographic data on the α_2 and β phases of Ti_3Al-based alloys in the literature [25, 29, 34, 35], $(\Delta V/V)_{\alpha_2/\beta}$ determined from these data are widely scattered (because the β and B2 phases are volume-

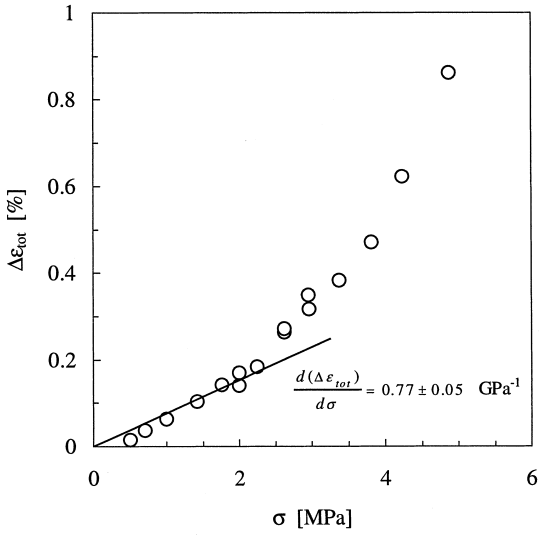

Fig. 5. Stress dependence of superplastic strain per half-cycle, $\Delta\varepsilon_{tot}$, of Super α_2 for cycles between 950 and 1150°C and frequency ν = 10/h.

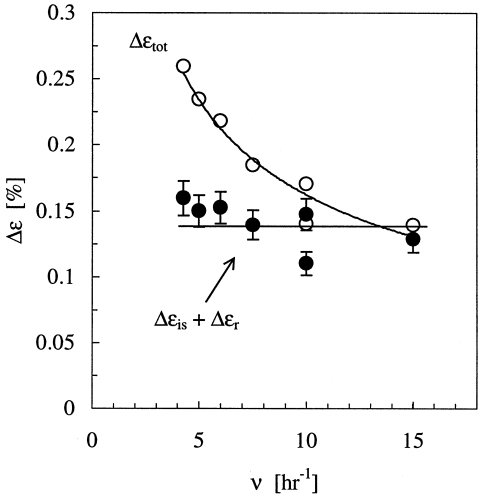

Fig. 7. Superplastic strain increment per α_2/β transformation as a function of cycling frequency, ν, for cycles between 950 and 1150°C with σ = 2.0 MPa. Empty circles are the total measured strain increments, $\Delta\varepsilon_{tot}$, and solid circles are the cycling strain increments due to internal stress and thermal ratcheting, $\Delta\varepsilon_{is} + \Delta\varepsilon_r$.

trically nearly identical [34], the combination β/B2 is denoted by β, here and below). Since an average bulk value for $\Delta V/V$ is needed for the continuum-mechanics models of transformation superplasticity [equations (1) and (2)], measurement of macroscopic dilatation during transformation is preferred. The length change due to phase transformation, $|\Delta L/L|_{\alpha_2/\beta}$ is determined from Fig. 2 to be $0.32 \pm 0.01\%$. Assuming that this represents a complete transformation from α_2 to β, the volume mismatch between these phases is thrice the length change during transformation, $|\Delta V/V|_{\alpha_2/\beta} = 0.96\%$.

The measured CTE of Super α_2, $\alpha_{75\text{–}450°C} = 1.00 \times 10^{-5}$/K, is in fair agreement with numerous studies of stoichiometric α_2 Ti_3Al ($9.5\text{–}12 \times 10^{-6}$/K) [36–39]. However, because Super α_2 often contains retained β in the temperature range of interest, direct comparison between these alloys is not possible. The data of Liao *et al.* (Fig. 2) provide the CTE of the β phase, $\alpha_\beta = 1.98 \times 10^{-5}$/K.

During thermal cycling, internal stresses are produced not only by the α_2/β phase transformation, but also by the thermal expansion mismatch

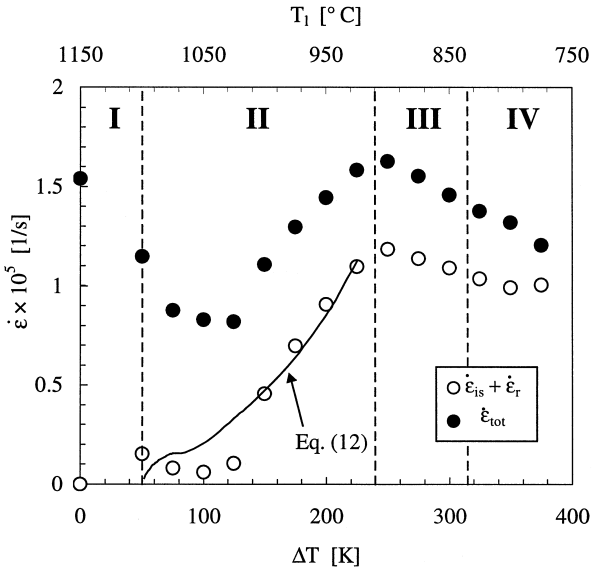

Fig. 6. Effective cycling strain rate as a function of cycling amplitude ΔT for cycling frequency ν = 10/h, upper temperature T_u = 1150°C, and applied stress of 2.6 MPa. T_l is the lower cycling temperature. Total effective strain rate, $\dot{\varepsilon}_{tot}$ (filled circles) as measured, and rate due only to internal stress and thermal ratcheting contributions, $\dot{\varepsilon}_{is} + \dot{\varepsilon}_r$ (open circles) are plotted with predictions of equation (12) in region II. T_l is the lower cycling temperature.

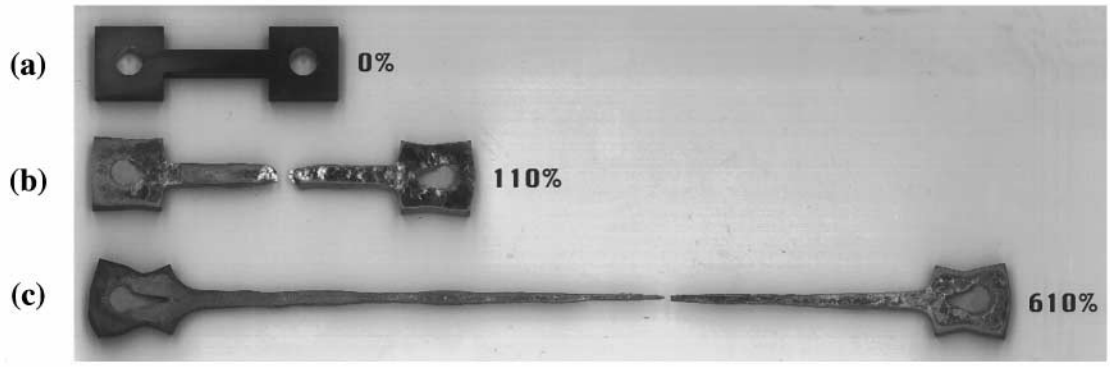

Fig. 8. Super α_2 tensile specimens: (a) in the undeformed state; (b) isothermally crept to failure at 1150°C and σ = 3.0 MPa; (c) thermally cycled between 950 and 1150°C, ν = 10/h, initial stress σ = 3.0 MPa.

between these two phases, which coexist for much of the cycle. Transformation superplasticity and other forms of internal-stress superplasticity are mechanically similar. Thus an effective CTE volume mismatch over a half-cycle can be defined as [40]:

$$\left|\frac{\Delta V}{V}\right|_{\mathrm{CTE}} = 3 \cdot \int_{\Delta T_{\mathrm{pl}}} G(f) \cdot \Delta\alpha \cdot \mathrm{d}T \qquad (6)$$

where $G(f)$ is a term accounting for the phase volume fraction f, $\Delta\alpha$ is the difference between the linear CTE of the two phases, and ΔT_{pl} is the temperature interval over which the internal stresses generated by the CTE mismatch produce plastic strains. For the temperature cycles applied to Super α_2 in this study, the volume fraction of the α_2 phase is a function of temperature dictated by the equilibrium thermodynamics of the system. In contrast to other investigations of internal-stress superplasticity (e.g. Refs [40, 41]), $G(f)$ is a function of temperature for the present thermal cycles, so this term must be evaluated in the integrand. Pickard and Derby [42] have modeled the volume fraction term of equation (6) as:

$$G(f) = f \cdot (1 - f) \qquad (7)$$

for the case where deformation occurs only in the weak phase. The creep data of Figs 3 and 4 indicate that this is a reasonable assumption for Super α_2, where deformation of the weak β phase is much faster than that of the two-phase $\alpha_2+\beta$ material. An average CTE mismatch $\Delta\alpha = 5.8 \times 10^{-6}$/K is found by taking an average of the literature values for the CTE of α_2 phase Ti_3Al at temperatures near the transformation [36–39], $\alpha_{\alpha_2} = 1.4 \times 10^{-5}$/K, and the CTE of the β phase determined from Fig. 2 ($\alpha_\beta = 1.98 \times 10^{-5}$/K). Equilibrium volume fractions of the α_2 phase with respect to temperature are given by Refs [23, 25], which can be fitted with a polynomial for the purposes of numerical integration. The range of integration, ΔT_{pl}, can be assumed to span the entire transformation range for a system relaxing stresses by creep, i.e. between the lower cycle temperature, T_{l}, and the β-transus, 1100°C. Introducing equation (7) into equation (6) with these values and assumptions yields $|\Delta V/V|_{\mathrm{CTE}} = 0.044\%$ for a half-cycle between 950 and 1150°C. The volume mismatch due to transformation over the same temperature range is $|\Delta V/V|_{\alpha_2/\beta} = 0.490\%$, given that only about 51% of the β is transformed to α_2 phase [23, 25]. Although smaller than the transformation volume mismatch, $|\Delta V/V|_{\mathrm{CTE}}$ is not negligible, and can contribute significantly to internal stress generation during thermal cycling.

On heating, the transformation and CTE mismatches tend to put the weak β phase in states of tension and compression, respectively. Thus the sign of these volume mismatches are opposite, and the effective volume mismatch $|\Delta V/V|_{\mathrm{eff}}$ is determined by:

$$\left|\frac{\Delta V}{V}\right|_{\mathrm{eff}} = \left|\frac{\Delta V}{V}\right|_{\alpha_2/\beta} - \left|\frac{\Delta V}{V}\right|_{\mathrm{CTE}}. \qquad (8)$$

For the values of transformation and CTE mismatch calculated above, equation (8) gives $|\Delta V/V|_{\mathrm{eff}} = 0.45\%$.

4.2. Isothermal creep

The creep behavior of Super α_2 (Fig. 3) in the β phase over the range T = 1100–1173°C is indicative of a transition between creep mechanisms. The observed increase of the stress exponent from 2.4 to 3.4 most likely represents a transition from diffusional creep ($n \approx 1$–2) at the lower temperatures to power-law creep ($n \approx 5$). At temperatures below the β-transus between 950 and 1050°C (Fig. 4), the stress exponent of unity indicates deformation by diffusional creep. This is consistent with reports on creep behavior of α_2 titanium aluminides at lower temperatures (500–900°C) and low stresses (20–200 MPa) which have identified a transition between power-law and diffusional creep [30, 31, 43]. Based on the activation energies for diffusion of titanium, Mishra and Banerjee [30] have noted that the creep behavior at these temperatures is grain-boundary diffusion controlled.

The activation energy of 300 kJ/mol [Fig. 4(b)] is in agreement with literature values (305–330 kJ/mol) [31, 42, 43] for dislocation creep with a lath-like or Widmanstätten morphology of α_2 phase [Fig. 1(b)]. Furthermore, the measured creep activation energy is close to the activation energy for volume diffusion of Super α_2 (330 kJ/mol [24]), and significantly different from that for grain boundary diffusion (202 kJ/mol [24]). Thus, we can conclude that creep is bulk diffusion-controlled, i.e. Nabarro-Herring creep. Considering that a Coble-creep regime has been identified between 575 and 725°C in Ref. [30], we can infer the presence of a transition between Coble and Nabarro-Herring deformation mechanisms at a temperature between about 725 and 950°C.

4.3. Thermal cycling

4.3.1. Contributions to deformation during cycling. The strain increment measured on each transformation ($\Delta\varepsilon_{tot}$) is composed of four contributions: those of transformation plasticity ($\Delta\varepsilon_{\alpha_2/\beta}$), CTE mismatch plasticity ($\Delta\varepsilon_{CTE}$), thermal ratcheting ($\Delta\varepsilon_r$), and creep caused only by the external biasing stress ($\Delta\varepsilon_{creep}$):

$$\Delta\varepsilon_{tot} = \Delta\varepsilon_{\alpha_2/\beta} + \Delta\varepsilon_{CTE} + \Delta\varepsilon_r + \Delta\varepsilon_{creep}. \quad (9)$$

Since the first two contributions are of a similar mechanical nature, they can be combined [equation (8)] into a single strain increment due to internal stress, $\Delta\varepsilon_{is}$. The remaining two contributions due to thermal ratcheting and creep caused only by the external stress are not considered in the continuum mechanics-based models of internal stress superplasticity [equations (1) and (2)], which are derived independently of the thermal cycle shape and frequency. Comparison between the experimental data and model predictions thus requires isolation of $\Delta\varepsilon_{is}$ from $\Delta\varepsilon_{tot}$, as described in the following sections.

4.3.1.1. Creep due only to applied stress

The creep strain accumulated during a half-cycle can be determined by integration of the operative creep law over the time of the half-cycle during which there is no phase transformation:

$$\Delta\varepsilon_{creep} = \int_{\Delta t} K \cdot \sigma^n \, dt. \quad (10)$$

The variable K is a function of temperature, which is related to time by the thermal cycle profile. The continuum-mechanics models of transformation superplasticity [equations (1) and (2)] consider creep of the material during the phase transformation. Because creep occurring independently of the transformation (i.e. outside the transformation temperature range) is not considered, the integration time, Δt, in equation (10) represents portions of the thermal half-cycle over which there is no phase transformation. However, in the present study it is very difficult to precisely determine the time during which the transformation enhances deformation, so the duration of the half-cycle, $t_{1/2}$, is used for Δt, resulting in an upper-bound value for $\Delta\varepsilon_{creep}$. For triangular thermal cycles which can be described by linear equations, equation (10) can be integrated in closed form [16, 44]. For the nearly square cycles of the present work, the most accurate course is direct numerical integration of the creep law over the experimentally-measured temperature profile. The creep strain rate is integrated piece-wise for sections above and below the β-transus, for which the creep laws of equations (4) and (5) are operative, respectively. The variables n and K [both functions of temperature in the β-field (Fig. 3)] and the time–temperature relationship of the thermal cycle are introduced into equation (10), which is then numerically integrated. By subtracting the integrated value ($\Delta\varepsilon_{creep}$) from the measured half-cycle strain ($\Delta\varepsilon_{tot}$), the strain increment due to internal stresses and thermal ratcheting ($\Delta\varepsilon_{is} + \Delta\varepsilon_r$) is recovered [equation (9)].

For steady-state thermal cycling-creep of a material with no phase transformation, $\Delta\varepsilon_{creep}$, as determined by this procedure is as accurate as the creep law and the mathematical description of the thermal cycle. For piece-wise integration across a phase-transus as performed here, equilibrium creep behavior (i.e. equilibrium microstructure) is assumed at every temperature in the cycle; kinetically-metastable microstructures are not considered. By comparing the predictions of the creep models of equations (4) and (5) with the experimental creep data and by considering the error in using $t_{1/2}$ in place of Δt, $\Delta\varepsilon_{is} + \Delta\varepsilon_r$ as determined by the method above is estimated to have uncertainty of about $\pm 8\%$.

4.3.1.2. Thermal ratcheting

When a sharp phase transformation front propagates through a material, macroscopic plastic deformation occurs in dimensions normal and parallel to the front, even in the absence of applied stress [8, 9]. In the present case, where heating is normal to the tensile direction, the phase front is expected [9] to propagate in directions normal to the gauge surface. Since the α_2 phase has higher strength and higher specific volume than the β phase, thermal ratcheting is expected to result in lengthening of the specimen in the tensile direction, as shown schematically in Fig. 9(a). Conservation of volume during ratcheting requires that the sample contract in the two dimensions normal to the tensile axis in this case.

Figure 10(a) shows ($\Delta\varepsilon_{is} + \Delta\varepsilon_r$) isolated from $\Delta\varepsilon_{tot}$ (Fig. 5) by the method described in the previous section. The low-stress data of this figure can be modeled by equation (1), which is linear with an intercept of zero. However, linear least-squares fitting of the data below 2.1 MPa indicates an ex-

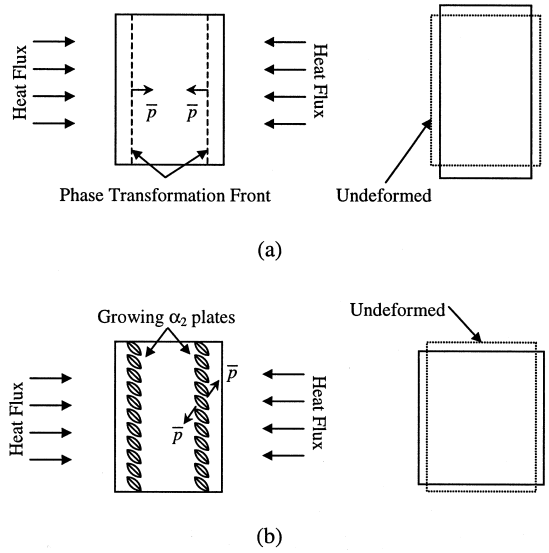

Fig. 9. Schematic representations of thermal ratcheting mechanisms: (a) the β/α_2 transformation front travels along the direction $\bar{p}$, parallel to the direction of heat flux (left), resulting in lengthening of the specimen in the gauge dimension (right) (mechanism described in Ref. [9]), and (b) proposed mechanism in which α_2 laths form in a single crystal and with a crystallographic relationship to the β phase (left). A macroscopic front of nucleation propagates in the direction of the heat flux, but local growth of α_2 plates proceeds in the $\bar{p}$ direction with a significant component in the gauge direction, resulting in a net shortening of the gauge (right).

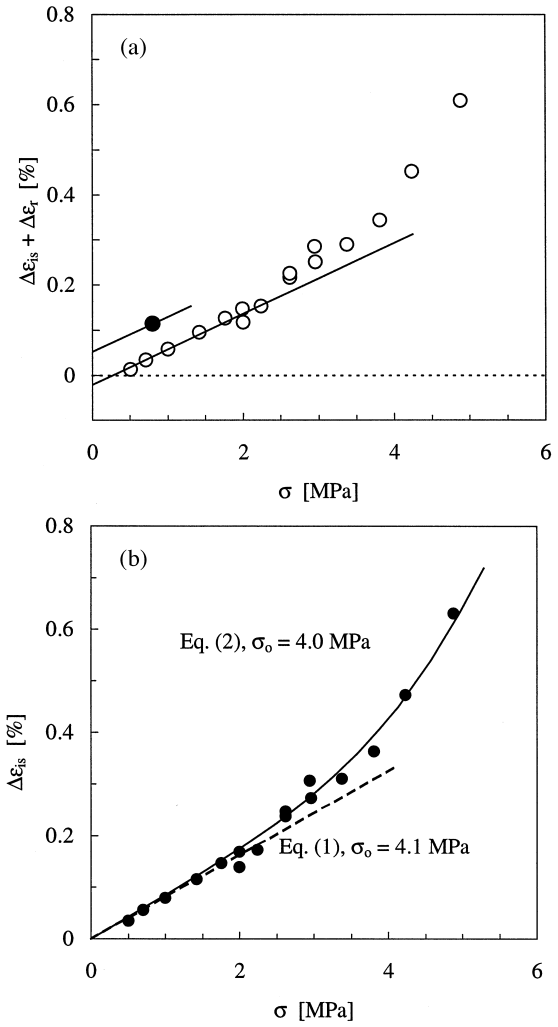

Fig. 10. Stress dependence of half-cycle strain increments during thermal cycling between 950 and 1150°C, v = 10/h: (a) cycling strains without creep for samples with the rolling direction oriented along the tensile axis (open circles) and perpendicular to the tensile axis (filled circle); (b) $\Delta\varepsilon_{is}$ fitted to the linear Greenwood and Johnson model [equation (1)] [3] and the nonlinear extension of this model [equation (2)] [10].

trapolated negative strain increment on each half-cycle due to thermal ratcheting, $\Delta\varepsilon_r = -0.020\%$. This result is not consistent with Fig. 9(a), which predicts a positive value of $\Delta\varepsilon_r$ if the transformation front propagates normal to the tensile axis. A possible explanation is that although nucleation of α_2 proceeds in directions parallel to the heat flux, the local transformation front does not necessarily travel in the same direction as heat flow, due to crystallographic constraints on the growth of α_2 plates or laths. The α_2 phase is known to form with $(0001)_{\alpha_2} \| \{110\}_\beta$, $\langle 11\bar{2}0\rangle_{\alpha_2} \| \langle 1\bar{1}1\rangle_\beta$ relations to the β phase [28], and rolled foils of Super α_2 have been shown to exhibit appreciable texture [22, 23]. Because the α_2 phase takes a lath or Widmanstätten morphology when cooling from above the β-transus [Fig. 1(b)], the orientation of local ratcheting strains are highly dependent on crystallographic orientation and growth direction of these laths. The presence of texture, therefore, could result in local transformation fronts propagating in directions with a component along the tensile axis. Fu *et al.* [23] have observed that rolled foils of Super α_2 have a majority of β {100} planes either oriented in the rolling plane or at 45° to the rolling plane, and it has been noted in Ref. [28] that the midribs of α_2 plates form parallel to the β {112} planes in other α_2 aluminides. If most of the growth of the α_2 phase occurs by thickening from the midrib, then the phase transformation front travels in a direction with a significant component along the rolling direction. As in Fig. 9(a), volume conservation during the ratcheting deformation requires a contraction in the direction along which the phase front propagates. In this manner, thermal ratcheting can result in shortening of the gauge length. A simple schematic of this ratcheting mechanism is depicted in Fig. 9(b) for a single crystal. In a polycrystalline sample the mechanism is operative in each grain, and texture provides a net preference for the local front propagation direction, $\bar{p}$, to have a component along the tensile axis.

The proposed ratcheting mechanism was investigated by thermally cycling a specimen machined with its gauge section perpendicular to the rolling

direction under a stress of 0.8 MPa, the result of which is shown in Fig. 10(a). Extrapolation by the same superplastic slope as for the previous samples reveals that with no applied stress, there is a positive plastic strain of 0.05% per transformation for the specimen with the gauge section machined normal to the rolling direction. This indicates that the transformation front tends to propagate with a strong component in the rolling direction, even when it is not coincident with the direction of heat flux. It can be concluded, therefore, that the texture of the tensile specimens oriented along the rolling direction is responsible for the unexpected negative ratcheting strains observed in Fig. 10(a).

The ratcheting mechanism depicted in Fig. 9(b) is further validated by the work of Furushiro *et al*. [45], who investigated transformation superplasticity of rolled commercially-pure titanium plates. For samples with the gauge parallel to the short- and long-transverse dimensions of the plate, they recorded elongations of 0.023 and 0.029%, respectively, after a complete thermal cycle about the transformation range of titanium with no applied stress. This result is in agreement with expectations based on the relative strengths and specific volumes of the two phases and the ratcheting mechanism of Fig. 9(a). A specimen with the rolling direction along its longitudinal axis exhibited contraction of 0.051% for a complete thermal cycle under no applied stress, consistent with the ratcheting behavior observed in the present study. Furushiro *et al*. [45] noted that the growth of α titanium occurs with a crystallographic orientation to the β phase, and that their specimens likely exhibited texture, but they did not identify thermal ratcheting as a cause of net deformation in the absence of applied stress.

Assuming that ratcheting strains are independent of applied stress for a given thermal cycle, $\Delta\varepsilon_r$ and $\Delta\varepsilon_{creep}$ can be subtracted from the measured strain increments $\Delta\varepsilon_{tot}$ [equation (9)], isolating the strain contribution due solely to transformation and CTE mismatch stresses, $\Delta\varepsilon_{is}$ [Fig. 10(b)].

4.3.2. Stress dependence of cycle strains. Figure 10(b) shows $\Delta\varepsilon_{is}$, isolated from $\Delta\varepsilon_{tot}$ of Fig. 5 by the methods described above. Both Greenwood and Johnson's model [equation (1)] and Mitter's extension of the model [equation (2)] assume that internal stresses generated by phase transformation or CTE mismatch are quickly relaxed by creep with a stress exponent, n. This parameter is difficult to assign for the case of Super α_2, as it varies from 1 to 3 over the cycling temperature range [Figs 3 and 4(a)]. As previously discussed, we can assume that internal stresses are relaxed only by creep of the weak β phase. Then, an average value of $n = 2.65$ is found by considering the measured stress exponent [Fig. 3(b)] over the portions of the cycle above the β-transus and by assuming that this value accurately describes the average creep behavior of the β phase over the entire thermal cycle. Because the predictions of equations (1) and (2) are insensitive to small changes in n [7], the averaging procedure above is reasonable. Taking the effective volume mismatch due to both transformation and CTE mismatch calculated earlier ($|\Delta V/V|_{eff} = 0.45\%$) and the above average stress exponent, the data of Fig. 10(b) can be fitted with equation (1) by a least-squares method in the low-stress regime where the model is valid. This procedure results in a value for the internal stress variable $\sigma_o = 4.1$ MPa.

A similar procedure can be followed with the model of equation (2), which is valid over the entire stress range. Because the volume integral of equation (2) is not analytically soluble, fitting is performed numerically in an iterative fashion over σ_o until the square error between experimental and modeled values of $\Delta\varepsilon_{is}$ is minimized. Employing the same values for $|\Delta V/V|_{eff}$ and n, equation (2) is best fitted to the experimental data with $\sigma_o = 4.0$ MPa [Fig. 10(b)], very close to the internal stress determined from the linear Greenwood and Johnson model ($\sigma_o = 4.1$ MPa). Because these two models have been independently fitted to data over different stress ranges, the good agreement between the two values of σ_o is encouraging.

Zwigl and Dunand [40] noted for the case of materials relaxing mismatch stresses by plastic yield that the linear model of Greenwood and Johnson is valid at applied stresses higher than those given by its specified range of validity ($\sigma \ll \sigma_y$, the yield stress of the weaker phase). Figure 10(b) illustrates that the same is true of a material relaxing by creep, as the linear model [equation (1)] is almost coincidental with the extended model [equation (2)] for stresses up to about $1/2 \cdot \sigma_o$. The data in the high stress regime deviate significantly from linearity, and can be well fitted with the extended, nonlinear model proposed by Mitter [10] [equation (2), Fig. 10(b)]. Although several studies have noted this nonlinear behavior for materials relaxing transformation stresses by creep [3, 7], the present work represents the first validation of the extended model to stresses greater than σ_o.

The internal stress can also be determined in the manner of Greenwood and Johnson [3] by considering the creep of the material during the phase transformation, from which they derived the following expression:

$$\sigma_o = \left[\frac{2}{3} \cdot \left|\frac{\Delta V}{V}\right|_{eff} \cdot \frac{1}{\Delta t^*} \cdot \frac{1}{K}\right]^{1/n} \qquad (11)$$

where K and n are given in equation (4) and Δt^* is the transformation time. For the cooling half-cycles of Super α_2, we take the transformation time given by the isothermal transformation diagram of Ref. [28] as $\Delta t^* \approx 110$ s at 950°C. Since we have assumed that creep occurs only in the weak β phase, the creep variables K and n in equation (11) are average values for the β phase over the half-

cycle. Therefore, the same average $n = 2.65$ found above and the corresponding average $K_\beta = 5.33 \times 10^{-7}$ [Fig. 3(b)] are appropriate for determination of the internal stress in the β phase. Using these values and $|\Delta V/V|_{\text{eff}} = 0.45\%$ as above, the internal stress is found to be $\sigma_o = 4.4$ MPa with equation (11). This value is in good agreement with the experimentally determined values, $\sigma_o = 4.0$ and 4.1 MPa.

In this approximation the variable Δt^* based on the cooling half-cycle is used, but the average internal stress, σ_o, should be representative of both heating and cooling half-cycles. The transformation of α_2 to β on heating half-cycles is most likely faster than the transformation on cooling, so the value of Δt^* employed above is probably overestimated. However, the sensitivity of equation (11) to changes in Δt^* is small; in the extreme case where the transformation on heating is instantaneous, the average transformation time is $\Delta t^* = 55$ s, and the internal stress is found to be $\sigma_o = 5.7$ MPa, still in reasonable agreement with the experimentally-determined 4.1 MPa.

4.3.3. Cycling amplitude. Figure 6 shows effective cycling strain rates $\dot{\varepsilon}_{\text{tot}}$ and $(\dot{\varepsilon}_{\text{is}} + \dot{\varepsilon}_{\text{r}})$ plotted as a function of cycling amplitude, ΔT, with an upper cycling temperature of 1150°C. The β-transus occurs at an amplitude $\Delta T \approx 50$ K, amplitudes below which there is no transformation and $\dot{\varepsilon}_{\text{tot}} = \dot{\varepsilon}_{\text{creep}}$ (marked as region I on Fig. 6). The isothermal transformation characteristics of Super α_2 [28, 29] indicate that cycles about the β-transus up to $\Delta T = 225$ K (region II on Fig. 6) result in direct transformation of β to α_2. The increase of $(\dot{\varepsilon}_{\text{is}} + \dot{\varepsilon}_{\text{r}})$ in region II can be considered in the framework of Greenwood and Johnson's model by introducing equation (11) into equation (1) and substituting $\dot{\varepsilon}_{\text{is}} = 2 \cdot \Delta\varepsilon_{\text{is}} \cdot \nu$ to obtain

$$\dot{\varepsilon}_{\text{is}} = 2 \cdot \nu \cdot \sigma \cdot \left(\frac{5 \cdot n}{4 \cdot n + 1}\right) \cdot (K \cdot \Delta t^*)^{1/n} \cdot \left(\frac{2}{3} \cdot \left|\frac{\Delta V}{V}\right|_{\text{eff}}\right)^{(n-1)/n}. \quad (12)$$

In the present case, frequency $\nu = 10$/h and applied biasing stress $\sigma = 2.6$ MPa are constant, and the stress exponent for creep of the weak β phase, $n = 2.5$, is assumed to be constant over the thermal cycles in region II (Fig. 6). The creep parameter K, the transformation time Δt^*, and the effective volume mismatch $|\Delta V/V|_{\text{eff}}$ are all functions of thermal cycle amplitude, ΔT. For a given ΔT, isothermal transformation times from Ref. [28] are taken for Δt^*, and $|\Delta V/V|_{\text{eff}}$ is determined according to the equilibrium phase fraction data of Refs [23, 25] following the procedures described earlier. The parameter K in equation (12) is approximated by averaging its values at the upper cycling temperature, $T_u = 1150$°C [Fig. 3(b)], and the lower cycling temperature, $T_l = T_u - \Delta T$, because (i) the contributions $\Delta\varepsilon_{\text{is}}$ for the α_2/β and β/α_2 transformations are assumed equal, and (ii) with nearly square thermal cycles, the transformations can be considered approximately isothermal at the upper and lower cycling temperatures. The value of K at the lower cycling temperature is determined by extrapolating the β phase creep data in the range 1100–1135°C to temperatures below the β-transus by an Arrhenius relationship. Between 1100 and 1135°C the stress exponent, n, is approximately constant [Fig. 3(b)] and the apparent activation energy, $Q_{\text{app}} = 573$ kJ/mol is found for data at $\sigma = 2.45$ MPa, close to the stress of the data in Fig. 6, $\sigma = 2.6$ MPa. The unphysically large value of activation energy is due to the change of dominant deformation mechanism between 1100 and 1173°C (Fig. 3).

Since all of the variables in equation (12) have been experimentally determined, the model is predictive without adjustable parameters across region II. As shown in Fig. 6, the agreement between the model predictions of $\dot{\varepsilon}_{\text{is}}$ and the experimental data for $(\dot{\varepsilon}_{\text{is}} + \dot{\varepsilon}_{\text{r}})$ is good. Since the contribution of thermal ratcheting is small compared to the internal stress contributions at high stresses [Fig. 10(a)], it is negligible for the purposes of comparison to the predictions of equation (12) in Fig. 6.

On cooling half-cycles from 1150°C with $\Delta T > 225$ K, the β phase undergoes a martensitic-like transformation to the orthorhombic O phase, which decomposes into α_2 after longer isothermal treatment [28]. Because of uncertainty in the isothermal transformation data, the microstructural evolution of specimens cycled with $\Delta T = 250$–300 K (inclusive) is largely unknown (region III on Fig. 6). However, for $\Delta T > 300$ K (region IV on Fig. 6) and cycling frequency $\nu = 10$/h, the isothermal transformation data [28] indicate that only the O phase was formed on cooling half-cycles. Since the volume fractions of O phase formed and $|\Delta V/V|_{O/\beta}$ are not known, quantitative analysis of these data is not possible. However, the decreasing trend through regions III and IV of Fig. 6 can be attributed to reduction in Δt^*, K, and/or $|\Delta V/V|$. Since the β/O reaction is described as martensitic-like [28], its transformation time is expected to be short compared to that of the β/α_2 transformation.

4.3.4. Cycling frequency. The strain increment due to internal stress and ratcheting, $\Delta\varepsilon_{\text{is}} + \Delta\varepsilon_{\text{r}}$, is shown along with $\Delta\varepsilon_{\text{tot}}$ as functions of ν in Fig. 7. Zwigl and Dunand [7] have identified several cycling frequency regimes for pure zirconium in which the superplastic strain increment on each half-cycle is dominated by a different contribution. For high cycling frequencies about the allotropic temperature of zirconium, they measured strain increments which were smaller than those predicted by continuum-mechanics models. They attributed the unexpectedly low strain increments to incomplete

transformations, restricted by the kinetics of heat transfer and phase transformation. This behavior is not observed for Super α_2 in the frequency range investigated, in agreement with the isothermal transformation characteristics of the alloy [28]. In order to investigate kinetically-limited partial cycling between α_2 and β, an apparatus capable of performing cycles at $\nu = 20/\text{h}$ and higher would be required [28]. At low frequencies, Zwigl and Dunand anticipated, but did not observe, that $\Delta\varepsilon_{tot}$ would increase as $1/\nu$, because the creep contribution to deformation becomes dominant. This behavior of $\Delta\varepsilon_{tot}$ is observed for Super α_2, and isolation of $\Delta\varepsilon_{is} + \Delta\varepsilon_r$ indicates that $\Delta\varepsilon_{creep}$ is the only contribution to deformation which is frequency dependent; the remaining contributions are, as expected, approximately constant across the frequencies investigated (Fig. 7).

5. CONCLUSIONS

High-temperature deformation of Super α_2 titanium aluminide has been investigated under both isothermal and thermal cycling conditions:

- Under an initial applied stress of 3.0 MPa, a tensile specimen cycled between 950 and 1150°C at frequency $\nu = 10/\text{h}$ failed after accumulating an engineering strain of 610%, compared with 110% for a control sample isothermally crept at 1150°C and 3.0 MPa. Microstructural superplasticity, which requires a fine, equiaxed microstructure, is ruled out in the present case due to a large β grain size and a lath-morphology of α_2 phase. To the best of our knowledge, this is the first demonstration of transformation superplasticity of an intermetallic compound.
- Because the α_2 and β phases coexist over a wide temperature range, internal stresses are generated not only by the phase transformation, but also by thermal expansion mismatch between the phases. This effect is modeled by calculating an effective volume mismatch due to both contributions. Introduction of this parameter into existing continuum-mechanics models results in an accurate description of stress-sensitivity of cycling strain increments for the entire range of stresses investigated.
- During cycling, thermal ratcheting contributes somewhat to deformation of Super α_2. The low stress data suggest that texture and crystallographically oriented growth of the α_2 phase combine to produce irreversible ratcheting contractions in the rolling direction.
- At low stresses during thermal cycling, the strain increment developed due to internal stress contributions over a single transformation is proportional to the applied stress, with an increasing stress sensitivity at higher applied stresses. By fitting the data to two existing models, the theoretical determination of the effective volume mismatch is validated, and the time- and space-averaged internal stress in the weaker β phase is found to be $\sigma_o \approx 4.0$ MPa.
- Variation in the thermal cycling amplitude results in different volume mismatches due to different equilibrium volume fractions of the transformation product. Superplastic strain increments are observed to increase with the fraction of α_2 phase formed. This effect is successfully modeled.
- Examination of superplastic strain increments as a function of cycling frequency reveals that the internal stress contributions to deformation are frequency-independent, but creep becomes dominant as the frequency is decreased.

Acknowledgements—This study was supported by the U.S. Army Research Office under grant DAAH004-95-1-0629 monitored by W. C. Simmons.

REFERENCES

1. Nieh, T. G., Wadsworth, J. and Sherby, O. D., *Superplasticity in Metals and Ceramics*. Cambridge University Press, Cambridge, 1997.
2. Dunand, D. C., in *International Conference on Thermomechanical Processing of Steels and Other Materials*, ed. T. Chandra and T. Sakai. TMS, Warrendale, Pennsylvania, 1997, pp. 1821–1830.
3. Greenwood, G. W. and Johnson, R. H., *Proc. R. Soc. Lond.*, 1965, **283A**, 403.
4. Zwigl, P. and Dunand, D. C., in *International Conference on Thermomechanical Processing of Steels and Other Materials*, ed. T. Chandra and T. Sakai. TMS, Warrendale, Pennsylvania, 1997, pp. 1831–1838.
5. Poirier, J. P., *J. geophys. Res.*, 1982, **87**, 6791.
6. Dunand, D. C. and Bedell, C. M., *Acta mater.*, 1996, **44**, 1063.
7. Zwigl, P. and Dunand, D. C., *Metall. Mater. Trans.*, in press.
8. Buckley, S. N., Harding, A. G. and Waldron, M. B., *J. Inst. Metals*, 1958, **87**, 150.
9. Stobo, J. J., *J. nucl. Mater.*, 1960, **2**, 97.
10. Mitter, W., *Umwandlungsplastizität und ihre Berücksichtigung bei der Berechnung von Eigenspannungen*. Gebr. Bornträger, Berlin, 1987, pp. 40–44.
11. Gautier, E., Simon, A. and Beck, G., *Acta metall.*, 1987, **35**, 1367.
12. Leriche, D., Gautier, E. and Simon, A., *Sixth World Conference on Titanium*, 1988, pp. 163–168.
13. Dunand, D. C. and Myojin, S., *Mater. Sci. Engng*, 1997, **230**, 25.
14. Zwigl, P. and Dunand, D. C., *Metall. Mater. Trans.*, 1998, **45**, 5285.
15. Johnson, C. A., Bradt, R. C. and Hoke, J. H., *J. Am. Ceram. Soc.*, 1975, **58**, 37.
16. Whitney, M. J., Transformation-mismatch plasticity in zirconia ceramic composites. M.S. thesis, Massachusetts Institute of Technology, Cambridge, Massachusetts, 1997.
17. Zwigl, P. and Dunand, D. C., in *Superplasticity and Superplastic Forming 1998, Supplemental Volume*, ed. A. K. Ghosh and T. R. Bieler. TMS, Warrendale, Pennsylvania, 1998, pp. 40–47.
18. Hornbogen, V. E. and Wassermann, G., *Z. Metallk.*, 1956, **47**, 427.

19. Liu, C. T. and Stiegler, J. O., *Metals Handbook: Properties and Selection: Nonferrous Alloys and Pure Metals*. American Society for Metals, Metals Park, Ohio, 1990, pp. 913–942.
20. Bassi, C., Peters, J. A. and Wittenauer, J., *JoMs*, 1989, **41**(9), 18.
21. Bassi, C. and Peters, J. A., *Scripta metall. mater*., 1990, **24**, 1363.
22. Albert, D. E. and Thompson, A. W., *Metall. Trans*., 1992, **23A**, 3035.
23. Fu, H. C., Huang, J. C., Wang, T. D. and Bampton, C. C., *Acta mater*., 1998, **46**, 465.
24. Pilling, J., Ridley, N. and Islam, M. F., *Mater. Sci. Engng*, 1996, **A205**, 72.
25. Jobart, D. and Blandin, J. J., *J. Mater. Sci*., 1996, **31**, 881.
26. Yang, H. S., Jin, P., Dalder, E. and Mukherjee, A. K., *Scripta metall. mater*., 1991, **25**, 1223.
27. Yang, H. S., Jin, P. and Mukherjee, A. K., *Mater. Sci. Engng*, 1992, **A153**, 457.
28. Ward, C. H., *Int. Mater. Rev*., 1993, **38**, 79.
29. Peters, J. A. and Bassi, C., *Scripta metall. mater*., 1990, **24**, 915.
30. Mishra, R. S. and Banerjee, D., *Mater. Sci. Engng*, 1990, **A130**, 151.
31. Cho, W., Thompson, A. W. and Williams, J. C., *Metall. Trans*., 1990, **21A**, 641.
32. Liao, B., Yang, K., Li, Y. Y., Wang, T. S. and Yuan, H., *Scripta metall. mater*., 1995, **32**, 277.
33. Frost, H. J. and Ashby, M. F., *Deformation-Mechanism Maps: The Plasticity and Creep of Metals and Ceramics*. Pergamon Press, Oxford, 1982.
34. Long, M. and Rack, H. J., *Mater. Sci. Technol*., 1995, **11**, 150.
35. Morris, M. A. and Morris, D. G., *Phil. Mag. A*, 1991, **63**, 1175.
36. Shashikala, H. D., Suryanarayana, S. V. and Murthy, K. S. N., *J. less-common Metals*, 1989, **155**, 23.
37. Zelenkov, I. A., Osipenko, I. A. and Osokin, E. N., *Poroshk. Metall*., 1976, **160**, 101.
38. Zelenkov, I. A. and Osokin, E. N., *Poroshk. Metall*., 1976, **158**, 44.
39. Gehlen, P. C., *Metall. Trans*., 1971, **2**, 1971.
40. Zwigl, P. and Dunand, D. C., *Acta mater*., 1997, **45**, 5285.
41. Kitazono, K., Sato, E. and Kuribayashi, K., *J. Jpn. Inst. Metals*, 1996, **60**, 441.
42. Pickard, S. M. and Derby, B., *Acta metall. mater*., 1990, **38**, 2537.
43. Hayes, R. W., *Acta metall. mater*., 1991, **39**, 569.
44. Kitazono, K. and Sato, E., *Acta mater*., 1998, **46**, 207.
45. Furushiro, N., Kuramoto, H., Takayama, Y. and Hori, S., *Trans. Iron Steel Inst. Japan*, 1987, **27**, 725.